Tethered networks in two dimensions: A low-temperature view

Paul E. Lammert*
Department of Physics, Simon Fraser University, Burnaby, British Columbia, Canada V5A 1S6

Dennis E. Discher
Departments of Mechanical Engineering and Applied Mechanics, Chemical Engineering, and Bioengineering, University of Pennsylvania, Philadelphia, Pennsylvania 19104

(Received 14 July 1997)

Perturbation theory and Monte Carlo simulation are applied to the study of low-temperature properties of a triangular phantom network of harmonic springs with nonzero resting length. We determine the equation of state and elastic moduli in the solid (ordered) phase, as well as the location of the solid-liquid phase boundary. A simple explanation is given for negative thermal expansivity. Agreement between two-loop perturbative results and simulation is fairly good, the largest discrepancies being in the location of the phase boundary. An expansion in inverse area, useful for the ordered phase, is also given. [S1063-651X(98)01104-0]

PACS number(s): 62.20.Dc, 64.60.Cn, 87.22.Bt, 05.20.−y

I. INTRODUCTION

Elastic lattices play a central role in a wide variety of problems in condensed matter. Among topics of current interest, we cite as illustration flux line arrays in type-II superconductors [1], charge-density waves [2], and tribology [3]. There are also a host of biological applications, such as the use of a *tethered network* as a model of the red blood cell cytoskeleton [4,5], which is a nearly perfect triangular network of spectrin filaments that fortifies the membrane at a low but nonzero effective temperature [6]. The present work is largely motivated by issues in the latter domain. Phenomenological descriptions in terms of an effective elastic Hamiltonian are often used [7] in these sorts of problems. The elastic moduli are unknown input and their variation with temperature is usually neglected.

To summarize this work, we bridge the gap to a macroscopic level by calculating elastic moduli for a particular model of the mesoscopic ball-and-spring variety. This provides an analytical point of reference complementary to Monte Carlo simulation, and we will see that straightforward two-loop perturbation theory gives good agreement on many quantitative details. We have extended previously published Monte Carlo simulations [8,9] in order to make that comparison.

Some variations on the theme are also considered. A resummed propagator can be used, but the results are not materially affected (see the end of Sec. IV). A ''quasivirial'' expansion is presented in Sec. VII, which does nicely for the well-ordered networks.

The approach taken here is an inherently low-temperature technique since it is based on perturbation theory around a perfectly ordered network. A tractable high-temperature complement is to be desired, of course. The permanent connectivity of the network seems, however, to frustrate the application of any traditional methods.

Unfortunately, we have not been able to incorporate self-avoidance (in the sense of Ref. [8]; see below) into the framework in a clean manner. Nevertheless, some lessons can be drawn concerning self-avoiding networks. In particular, it is now clear that self-avoidance begins to stabilize the network at temperatures significantly lower than naively expected (see Sec. VI). Bond-angle dependence could be added to the energy function, but it is unclear whether that is very satistfactory as the constraint one wants to model is rather singular. Finally, we remark that, at a mean-field level, a simple tension acts much like a self-avoidance constraint.

II. THE MODEL AND ITS PHASES

To be specific, the system studied is a triangular network, the Hamiltonian function of which is a sum of harmonic spring terms over nearest-neighbor pairs $\langle ij \rangle$:

$$V = \frac{K}{2} \sum_{\langle ij \rangle} (|\mathbf{r}_{ij}| - s_0)^2. \tag{1}$$

For most situations in which this model would be appropriate, V actually incorporates some entropy arising from microscopic degrees of freedom that do not appear explicitly in the description. Steric interactions between the tethers connecting nearest neighbors can be modeled by a *self-avoidance* constraint, which allows only configurations that can be produced by deformation of the reference configuration without passing any nearest-neighbor bond through another. The designation ''phantom'' refers to a network lacking such a constraint.

At low or negative pressure the ground state of the tethered net is an expanded regular (positionally ordered) triangular conformation possessing C_6 rotational symmetry. Fluctuations in the relative position of vertices i and j are measured by $\langle |\mathbf{u}_i - \mathbf{u}_j|^2 \rangle$ and of the relative orientations of nearest-neighbor bonds ij and kl by $\langle (\mathbf{u}_i - \mathbf{u}_j) \cdot (\mathbf{u}_k - \mathbf{u}_l) \rangle$, where $\mathbf{u}_i$ is the deviation of vertex i from its zero-temperature position. The former correlation function diverges as $T \ln|\mathbf{r}_i - \mathbf{r}_j|$, according to the arguments of the

*Present address: Department of Physics, The Pennsylvania State University, University Park PA 16802.

Mermin-Wagner-Coleman theorem [10]. This signals the destruction of long-range positional order by long-wavelength fluctuations to which bond-orientational order is immune. One therefore expects a bond-orientationally ordered, C_6-symmetric phase at low temperature and pressure.

Under sufficiently high pressure, the ground state of the *self-avoiding* network is a crushed one-dimensional structure. One side of each triangle is twice as long as the other two, so the symmetry group is reduced to C_2. Fluctuations are clearly suppressed in a way that invalidates the Mermin-Wagner argument. It is reasonable to suppose that there is a C_2-symmetric ordered phase at positive temperature. The phantom network, on the other hand, has no C_2-symmetric, ordered phase for $T>0$.

Notice that, since the transition between the C_6-symmetric phase and either a C_2 phase or a disordered phase implies spontaneous symmetry breaking, it *cannot* end in a critical point. Either both phases persist for all T or there is a third high-temperature phase (almost certainly fully disordered). It is not clear whether self-avoidance can maintain the order to arbitrarily high temperature.

In Monte Carlo simulation [8], phantom tethered networks were seen to suffer a first-order *collapse* transition from the C_6 phase to a disordered phase at a quite low temperature. Self-avoiding networks, by contrast, were later observed [8,9] to exhibit the above-noted first-order C_6 to C_2 transition, which persisted to the highest temperatures probed. The presence or absence of a third phase of the self-avoiding network was not definitively established. Other simulation efforts [11], report a critical point. In the common region of C_6 symmetry, the self-avoiding net behaves much like the phantom network. As will be shown, however, that region is rather small at low tension. This indicates that steric constraints are important at much lower temperatures than one might have supposed.

III. DEFORMATION, TENSION, AND ELASTIC MODULI

In the following, we make use of variables that have been made dimensionless by using s_0 and $Ks_0^2/2$ as length and energy units. The dimensionless temperature and pressure are

$$\tau \equiv \frac{k_B T}{K s_0^2/2},$$

$$p \equiv \sqrt{3}\,\frac{P}{K} = P\,\frac{A_0/N}{K s_0^2/2},$$

where A_0 is the area of the network at $T=P=0$ and N is the number of vertices. Other quantities that have been rendered dimensionless in this way, such as free energies and elastic moduli, are indicated by an overbar.

At zero temperature and pressure, the network forms a perfect triangular lattice of spacing one (s_0 in physical units). Under a global affine deformation described by a matrix M, the node originally at X_0 moves to $X=MX_0$. A convenient parametrization of the deformation matrix M [12] is (see Appendix A for details)

$$M = \begin{pmatrix} s+\phi_1 & \phi_2 \\ \phi_2 & s-\phi_1 \end{pmatrix}. \tag{2}$$

The symmetries of the hexagonal network allow a Fourier expansion of $F(M)$ in $\theta \equiv \arg(\phi)$ ($\phi=\phi_1+i\phi_2$):

$$\overline{F}(s,\phi) = \overline{F}(s,0) + \sum_{n\geqslant 0} f_n(|\phi|^2)\cos(3n\theta). \tag{3}$$

In the spirit of the Landau approach, one just takes the first few terms of the power-series expansions of the coefficient functions $f_n(x)$. At $T=0$, one gets simply the Taylor expansion of V:

$$\frac{1}{N}\,\overline{V}(M) = 3(s-1)^2 + \frac{3}{2}\left(2-\frac{1}{s}\right)|\phi|^2 - \frac{3}{8s^2}\,(\phi^3+\overline{\phi}^3) - \frac{3}{32s^3}\,|\phi|^4 + \cdots . \tag{4}$$

It is necessary to use the Gibbs free energy $G(p) = \inf_A[F(M)+PA]$ when the pressure is nonzero. The dimensionless area per vertex is $a=A/A_0=s^2-|\phi|^2$, so that $\overline{PA}/N=pa$. For a phantom network ''area'' is not an unambiguous concept; we must specify what it means. The area of an elementary triangle is a signed quantity. If the production of a conformation from the $T=P=0$ reference configuration involves changing the orientation of a triangle, i.e., a vertex passes through the opposite side, then that area is negative. Essentially, the two choices for A are either the total signed area or its absolute value.

We adopt here the point of view that A means the absolute value of the total (signed) area. This *unsigned total area* is different from the sum of unsigned areas of individual triangles, of course. If we conceive of periodic boundary conditions as involving configurations on an actual torus, then its real size is given by the unsigned total area. Since we work with a lattice of k points, periodic boundary conditions are implicit here.

Coupling pressure to the total signed area instead of its absolute value has significant consequences. The network will not maintain a positive area under *any* positive pressure; it tends to turn inside out. The part of the ordered phase in Fig. 1 at $p>0$ vanishes, reappearing at negative A. The phase diagram is symmetric about the line $A=0$. Finally, we comment that the possibility of neatly folded conformations, which do not affect the value of the elastic energy, might also eliminate this part of the (C_6-symmetric) ordered phase.

Bulk and shear moduli B and μ are obtained from the curvatures of the Gibbs free energy at its minimum,

$$\delta F + P\,\delta A \approx \sqrt{3}N[B(\delta s)^2 + \mu|\phi|^2]. \tag{5}$$

The Poisson ratio, defined as $\sigma=(B-\mu)/(B+\mu)$, measures the strain response of the system along some direction to a small externally applied strain in a perpendicular direction. If it is negative, under compression along one axis, the network contracts along the orthogonal direction. Boal, Seifert, and Shillcock [8] measured the Poisson ratio in simulations of a variety of tethered nets and found that it is generally negative at intermediate tensions, a finding that seemed to cause some

surprise when reported. A negative Poisson ratio is very unusual in real materials. The phantom tethered net has a negative Poisson ratio in almost the entire ordered phase (see Fig. 1).

IV. PERTURBATIVE SETUP

At zero temperature, nearest-neighbor separation vectors take the affinely distorted values $\mathbf{e}_{ij} \equiv M\mathbf{e}_{ij}^0$. Thermal fluctuations are described by the ''phonon'' variables

$$\mathbf{u}(\mathbf{k}) = \frac{1}{N^{1/2}} \sum_i e^{-i\mathbf{k}\cdot\mathbf{r}_i}\mathbf{u}_i ,$$

where $\mathbf{u}_i$ is the deviation of vertex i from its zero-temerature position. Thus (repeated indices are summed over)

$$\delta\overline{V} = \sum_{\mathbf{k}} \frac{1}{2}[G_0(\mathbf{k})^{-1}]^{\mu\nu}u(\mathbf{k})^{\mu}u(-\mathbf{k})^{\nu} + \sum_{n\geqslant 3} \frac{1}{n!} N^{1-n/2} \times \sum_{\{\mathbf{k}_i\}} \Phi_n(\mathbf{k}_1,\ldots,\mathbf{k}_n)^{\mu,\ldots,\nu}u(\mathbf{k}_1)^{\mu}\cdots u(\mathbf{k}_n)^{\nu}. \quad (6)$$

The real-space propagator G_0 is given by

$$[G_0^{-1}]^{\mu\nu}(\mathbf{e}) = 2\delta^{\mu\nu} - 2|\mathbf{e}|^{-1}(\delta^{\mu\nu} - \hat{e}^{\mu}\hat{e}^{\nu}), \quad (7)$$

where $\hat{e}$ is a unit vector along a nearest-neighbor bond $\mathbf{e}$. Expressions for the vertices Φ_n needed for our calculations, $3 \leqslant n \leqslant 6$, are given in Appendix B for the benefit of the interested reader.

The free energy is now written as $\overline{F(M)} = -\tau \ln\int [du] e^{-V/k_BT}$ and we calculate perturbatively in δV. Propagators and vertices in the Feynman diagrams carry factors of τ and τ^{-1}, respectively. Thus the relation $L = I - V + 1$ between the numbers L of loops, I of internal lines, and V of vertices shows that the number of loops is one greater than the number of powers of τ. The loop expansion is therefore a low-temperature expansion. We have carried the calculation only to two loops. One could go further, but not much, since the computational time required for calculation of a given correlation function grows at least as rapidly as N^L. There are 16 topologically distinct diagrams for the two-loop calculation. They are calculated at each lattice constant of interest, producing three quadratic polynomials in T. The calculations reported here were done on a 20×20 grid covering the first Brillouin zone in k space. The results are not materially affected by using a grid as small as 12×12.

It should be noted that the calculations discussed here are free of infrared difficulties. As $k \to 0$, the bare propagator behaves as $1/k^2$. However, vertices scale as $\Phi_n \sim k^n$. Since there are no genuine low-momentum external legs in our diagrams, these factors compensate precisely. In other words, we do not calculate correlation functions of u at large distances. As a consequence of this fact, it does not matter that we pretend the network possesses long-range translational order even though it is actually only *quasi-long-range*.

Some effects of higher orders in the perturbative expansion can be fairly easily tested by using a self-consistent resummed propagator in the diagrams, as we have done. Generally, the free energy does not lend itself well to resummation schemes [13]. The pressure and elastic moduli, however, are given by derivatives of $F(M)$ with respect to the elements of M, e.g.,

$$-p = \frac{1}{2s}\frac{\partial\overline{F}}{\partial s} = \frac{1}{2s}\left\langle \frac{\partial\overline{V}}{\partial s}\right\rangle ,$$

with $\partial/\partial s = \partial/\partial M_1^1 + \partial/\partial M_2^2$. Since these are essentially correlation functions, some resummations become feasible, though there is no compelling physical reason for such gymnastics.

The self-consistent propagator is calculated iteratively, the $(n+1)$st approximation to G^{-1} being determined from the nth via the recursion relation

$$G_{n+1}^{-1} = G_0^{-1} - \Sigma_n , \quad (8)$$

where Σ_n is the one-loop self-energy with G_n on the internal lines. There are then two graphs for Σ. In fact, using this G changes the results little, except very close to the phase boundary, which shifts a bit as a result. Since the results no longer take the form of polynomials in T when using the partially resummed propagator, one also has the significant drawback of needing to perform the calculations separately at each temperature of interest.

V. MONTE CARLO DETAILS

Simulations of periodic networks in $D=2$ at nonzero temperature and pressure or tension have been described extensively elsewhere [8,9]. In a single Monte Carlo step, each of N vertex particles is displaced randomly and a fluctuation in both the box dimensions and shape are attempted. Moves are accepted under a suitable Boltzmann weight and adjustments are made in order to maintain an acceptance rate near 40%. Figures 1–4 show Monte Carlo data points for the average area and elastic moduli, the latter from fluctuation formulas, for $N = 12^2$ networks. Networks of size 4^2, 6^2, and 24^2 were also examined under a tension $-p = 0.1$ and altogether display a $N^{-1/2}$ scaling for the temperature of transition from the expanded phantom network to a collapsed state. Based on this scaling, the location of the phase boundary is deemed accurate to within 15%. Further, the last several data points in a plotted series generally represent stable averages after order 10^7 Monte Carlo steps, an ensemble typically greater by a factor of 10 than the (unplotted) next point in the series.

VI. THERMAL EXPANSIVITY AND INSTABILITY

Another unusual feature of the phantom network is that the thermal expansivity is negative throughout the ordered phase. The self-avoiding network also exhibits this phenomenon at very low temperature [9]. Its departure from this behavior indicates that fluctuations are probing the steric constraints. As we now show, a negative thermal expansivity is easily understood and generally to be expected for interactions with no hard core.

In k space, the bare propagator (7) is

$$[G_0(\mathbf{k})^{-1}]^{\mu\nu} = 2\sum_e a_e\{\delta^{\mu\nu} - |\mathbf{e}|^{-1}\Pi_e^{\mu\nu}\}, \quad (9)$$

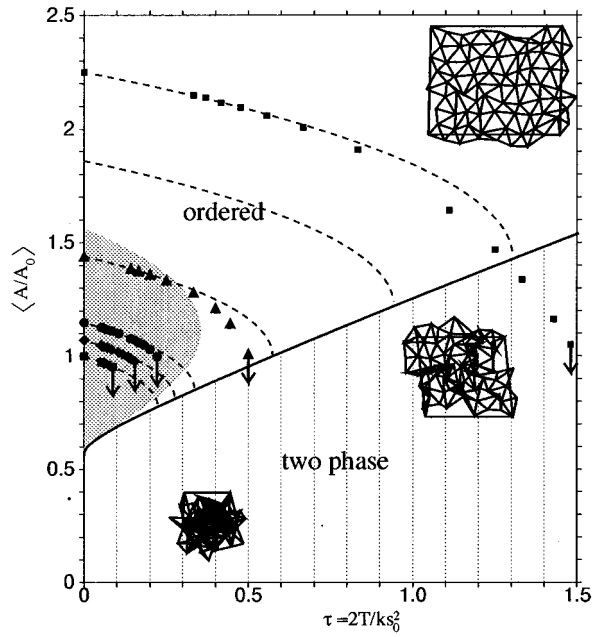

FIG. 1. Phase diagram in the A-T plane. Isobars are indicated by dashed lines at $-p=0$, 0.1, 0.2, 0.5, 0.8, and 1.0. Monte Carlo results along these isobars (except for $p=-0.8$) are plotted as data points. The points with arrows indicate the highest temperature at which the network was ordered. For the perturbative calculation, the phase boundary is defined by divergence of the compressibility. The shaded region indicates a positive Poisson ratio from the two-loop calculation. It does not actually touch the phase boundary except at $T=0$. The inset pictures are to give some impression of the conformations for expanded and collapsed nets. Their precise placement in the diagram has no significance.

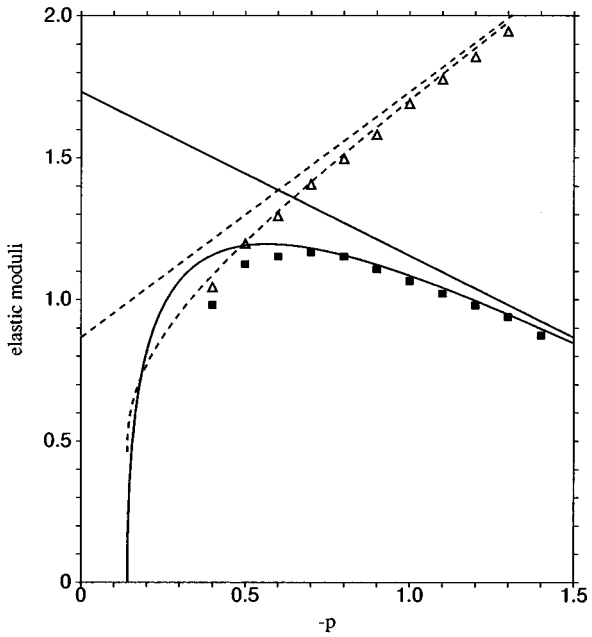

FIG. 2. Dimensionless bulk and shear moduli at $\tau=0.30$. Curved lines ($\overline{B}$ solid and $\overline{\mu}$ dashed) are from the two-loop calculation and the data points are Monte Carlo results (triangles for $\overline{\mu}$ and squares for $\overline{B}$). The straight lines are zero-temperature values for comparison. The shapes are similar for other temperatures.

where Π_e is a projector onto the line orthogonal to e and $a_e=4\sin^2(\mathbf{k}\cdot\mathbf{e}/2)\geqslant 0$. Remember that k is scaled with the lattice parameter s, so it is dimensionless and the entire collection of k vectors is independent of s. Eigenvectors of $G_0(k)$ are completely determined by the sum of projectors in Eq. (9), which is a positive operator and independent of s. Hence the eigenvectors are also independent of s and the associated eigenvalues are decreasing with s. (We might say that the mode-specific Grüneisen parameters are all negative, though this usually refers to genuinely fixed k.) Thus the harmonic fluctuation contribution to F is always decreased by contracting the lattice. This argument applies to any lattice structure in any dimension, requiring only a nearest-neighbor harmonic potential.

A more intuitive understanding can be obtained from simply thinking about the shape of the potential (1). The potential for longitudinal bond fluctuations is harmonic, so a slight increase in s is no better or worse than a slight decrease. In contrast, the curvature of the potential that is relevant for transverse fluctuations is less for $s<1$ than for $s>1$ because in the former case fluctuations bring the bond length back toward the minimum of the potential, but further away in the latter. With minor modifications, this argument seems to go through for other power-law potentials [e.g., $(s-1)^4$], which is nice, since even constructing a perturbation theory for such a case is rather delicate. The partition function of an isolated fluctuating triangle, as opposed to an entire network, can be calculated exactly [9]. That analysis demonstrates the same feature of a negative thermal expansion modulus.

In contrast to the total area, which is precisely $(\sqrt{3}/2)Ns^2$ by definition, bond lengths fluctuate. As a result, although the mean bond length decreases with rising temperature, it does so more slowly than the area.

A simple energy-entropy argument also gives an indication of the collapse transition. The key is the observation that

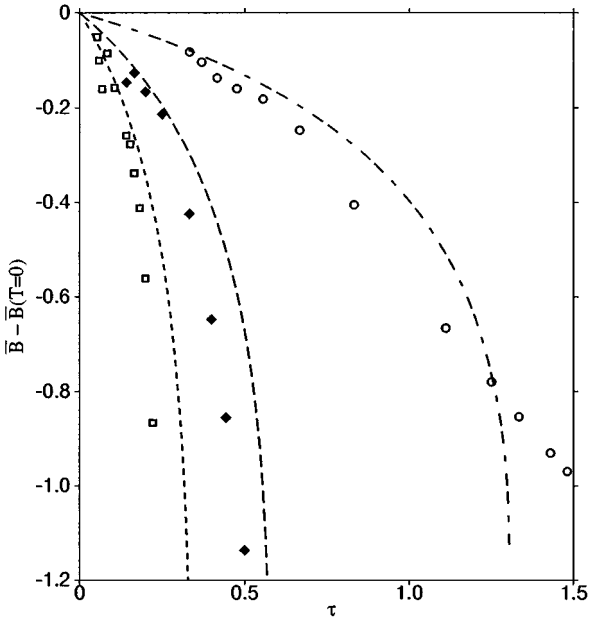

FIG. 3. Dimensionless bulk modulus $\overline{B}$ along isobars at $-p=0.2$ (open squares), 0.5 (closed diamonds), and 1.0 (circles), offset by the $\tau=0$ values. Data points are from Monte Carlo results and the lines are two-loop results.

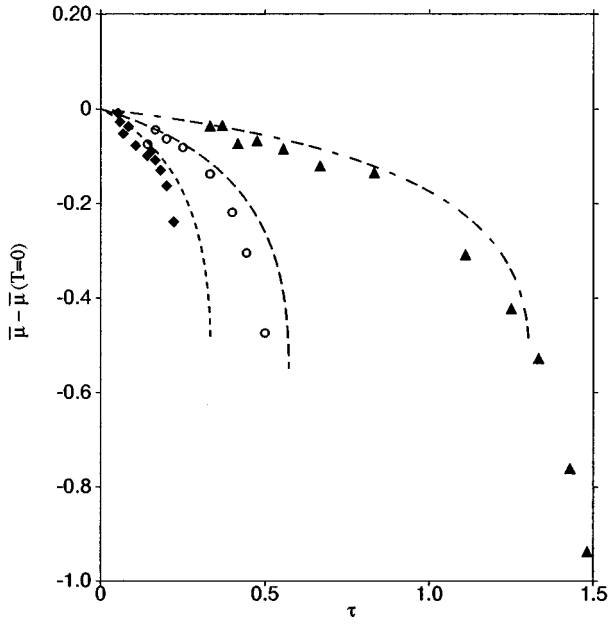

FIG. 4. Dimensionless shear modulus $\bar{\mu}$ along isobars at $-p=0.2$ (closed diamonds), 0.5, and 1.0, offset by zero-temperature values. Data points are Monte Carlo results and the lines are two-loop results.

the collapsed phase seems to develop as chains of collapsed triangles in an otherwise ordered network [8]. Such a chain can be visualized as a random walk on the dual lattice. The walk crosses one bond entering a triangle and another exiting. These two are collapsed to a length of approximately $s/2$, while the third maintains its length of s. Then, for each step of the walk there is an elastic energy gain $\delta E \approx (s/2-1)^2-(s-1)^2=s-3s^2/4$ from shrinking a bond and pressure-area work of about $-ps^2/2$ from the collapse of a triangle. Finally, each step of the walk entails a choice between two sides of a triangle, so there is an entropy of $\ln 2$ per step. These ingredients yield a condensation temperature for these linear ''defects,'' identified with the transition and given by

$$\tau^* \approx [s-(p/2+3/4)s^2]/\ln 2.$$

For fairly high tension, $p \to -3$, this says that, along the transition line, temperature essentially scales with area. Using the zero-temperature relation $s^{-1}=\delta p/3 \equiv 1+p/3$, we arrive at the crude estimate $T^* \approx 3[\frac{3}{2}-p]/[(3+p)^2 2\ln 2]$. This agrees with simulation results for the phase boundary to better than an order of magnitude for $0<-p<2.2$.

VII. 1/S EXPANSION

The perturbative calculations we have discussed require a separate calculation for each area. It is also possible to construct a double expansion in T and $1/s$, sort of quasivirial expansion. Since this requires just a handful of numbers, it gives ''more for less,'' when applicable. Expansion in $1/s$ is naturally suggested by the structure of the potential V. For $n \geqslant 3$, the vertex Φ_n scales as $s^{-(n-1)}$. The first term on the right-hand side of Eq. (7) is taken as a new bare propagator, which is then independent of s. The second term becomes an additional vertex Φ_2 and the scaling holds for this one as well. In this new scheme, any diagram for the free energy has a degree in s (denoted S, naturally), given by $-S=2(L-1)+V=L-1+\frac{1}{2}\Sigma n V_n$, where V_n is the number of vertices of order n. Thus only a finite number of vertices enter at any given order in s^{-1}. Furthermore, we obtain the inequalities $-S/2<L-1<-S$.

TABLE I. Coefficients of the expansion of p and $\bar{\mu}$ in powers of T and $1/s$, according to Eq. (10).

n	$p_{1,n}$ (10^{-3})	$\mu_{1,n}$ (10^{-3})	$p_{2,n}$ (10^{-3})	$\mu_{2,n}$ (10^{-3})
3	250	72.17	0	0
4	146.57	14.93	0	0
5	94.85	10.31	31.25	−9.02
6	64.70	8.49	40.60	−32.85
7	45.32	5.76	37.99	−55.40
8	32.20	3.16	31.70	−62.94

Writing the zero-temperature parts explicitly, we express the pressure and elastic moduli as

$$p=-3+3s^{-1}-\sum_{n,m\geqslant 1} p_{n,m}s^{-m}\tau^n,$$

$$\bar{B}=\sqrt{3}s^{-1}+\sum_{n,m\geqslant 1} b_{n,m}s^{-m}\tau^n,$$

$$\bar{\mu}=\sqrt{3}(2-\tfrac{3}{2}s^{-1})+\sum_{n,m\geqslant 1} \mu_{n,m}s^{-m}\tau^n. \qquad (10)$$

Values of the coefficients for $m \leqslant 8$ are given in Table I (bulk modulus coefficients are not tabulated since they are given by $b_{n,m}=-mp_{n,m}$). By setting $B=0$, the first two terms of that series suggest a transition temperature $T^* \sim s^2$, as did the energy-entropy argument of Sec. VI. Curiously, the numerical coefficients are in close agreement: 2.31 and 2.16. Unfortunately, although the two-loop phase boundary is quite straight, the slope is much smaller, and even smaller for simulations.

Deep in the ordered phase, the agreement between this expansion and the full two-loop calculation is very close. Deterioration of the agreement near the phase boundary leads to a non-negligible difference in its location.

VIII. DISCUSSION

Deep in the network's ordered phase, the agreement between Monte Carlo and two-loop perturbative results presented here is satisfying. The poor agreement on the location of the phase boundary, however, is somewhat disappointing. Since the perturbative calculations are essentially an expansion in T, this divergence at high temperature is not terribly surprising. On the other hand, the considerable discrepancy at very low temperature (i.e., *low tension*) is puzzling. Vaguely speaking, it may be that the perturbation theory misidentifies some sort of metastable state as the equilibrium phase. Despite this, emphasis is placed by both theory and simulation on the importance of steric interactions in stabili-

zation of a low-temperature Hookean spring model of the cytoskeleton.

The self-avoidance interaction we have discussed can be expressed as a limit of a term in the Hamiltonian that suppresses negative area. For example, the sum $\lambda\Sigma\theta(-A)$ of step functions on the elementary areas, as $\lambda\to\infty$, will work. In some ways, the network responds similarly to imposition of a tension and to a self-avoidance interaction, for example, in stabilization of the ordered phase. Perhaps the reason is a bit easier to see with our remark. An observation in a similar vein [14] is that the self-avoidance for a planar network can be recovered as the infinite bending-rigidity limit of a network free to fluctuate in more than two dimensions.

ACKNOWLEDGMENTS

During this work, P.E.L. was supported by NSERC of Canada. D.E.D. gratefully acknowledges computational support for simulations from the Laboratory for Research on the Structure of Matter at the University of Pennsylvania. Simulations were initiated at Simon Fraser University with the support of the U.S. National Science Foundation and the Canadian Institute for Advanced Research. This work was supported in part by the MRSEC Program of the National Science Foundation under Award No. DMR96-32598.

APPENDIX A: LATTICE SYMMETRY CONSIDERATIONS

Rotations in two dimensions are most easily discussed by using the complex coordinates $z\equiv x+iy$ and $\overline{z}\equiv x-iy$. We have

$$\begin{pmatrix} M_x^x & M_y^x \\ M_x^y & M_y^y \end{pmatrix} = \mathrm{Re}\begin{pmatrix} M_z^z+M_{\overline{z}}^z & i(M_z^z-M_{\overline{z}}^z) \\ -i(M_z^z+M_{\overline{z}}^z) & M_z^z-M_z^z \end{pmatrix} \quad \text{(A1)}$$

for the relation between the deformation matrix in the x,y and $z,\overline{z}$ bases.

As a function of the deformation M, the free energy exhibits both left and right rotational invariances: $F(R(\theta_l)MR(\theta_r))=F(M)$ for θ_l arbitrary, and $\theta_r\in(\pi/3)\,\mathbb{Z}$. Rotation simply changes the phases of z and $\overline{z}$, so, for example, $M_{\overline{z}}^z\mapsto e^{i(\theta_l-\theta_r)}M_{\overline{z}}^z$. Fix one $U(1)$ invariance by requiring that M_z^z be real (equivalent to $M_y^x=M_x^y$). There remains a symmetry under $\theta_l=-\theta_r=n(\pi/3)$, which is the C_6 symmetry of the lattice. $M_z^z\neq 0$ will indicate that this C_6 symmetry is broken. The notation used in the body of the paper is related by $s=2M_z^z$ and $\phi\equiv\phi_1+i\phi_2=M_{\overline{z}}^z$. In the $z,\overline{z}$ basis,

$$M=\begin{pmatrix} s & \phi \\ \phi^* & s \end{pmatrix}. \quad \text{(A2)}$$

The triangular lattice also has two inequivalent sets of reflection symmetries, which take the form $z\mapsto e^{-2i\varphi}\overline{z}$, where φ is the angle between the reflection axis and the x axis. With coordinates oriented so that the x axis is itself a reflection axis, the free energy is invariant under complex conjugation of M in Eq. (A2), i.e., under $\phi_2\mapsto-\phi_2$.

We may now attempt a Landau expansion of $F(M)$ about $\phi=0$, at fixed s. Writing $\phi=|\phi|e^{i\theta}$, monomials allowed by C_6 symmetry are of the form $|\phi|^{2m}$, $|\phi|^{2(m+n)}\cos(3n\theta)$, and $|\phi|^{2(m+n)}\sin(3n\theta)$. Reflection invariance eliminates those odd in θ, i.e., the sine terms.

APPENDIX B: INTERACTION VERTICES

The k-space vertices are obtained by Fourier transformation of their real-space counterparts

$$\Phi_n(k_1,\ldots,k_n)^{\mu,\cdots,\nu}=\delta\Big(\sum k_i\Big)\sum{}'\,\Phi_n^{\mu,\cdots,\nu}(\mathbf{e}) \times\prod\,[e^{i\mathbf{k}_i\cdot\mathbf{e}_0}-1],$$

where the sum runs over nearest-neighbor vectors $\mathbf{e}_0$ of the *undeformed* $(M=1)$ reference lattice. For $3\leqslant n\leqslant 6$, the real-space interaction vertices are

$$\Phi_3^{\mu\nu\lambda}(\mathbf{e})=\frac{6}{|\mathbf{e}|^2}\,[\,\delta^{(\mu\nu}\hat{e}^{\lambda)}-\hat{e}^{\mu}\hat{e}^{\nu}\hat{e}^{\lambda}],$$

$$\Phi_4^{\mu\nu\lambda\rho}(\mathbf{e})=\frac{6}{|\mathbf{e}|^3}\,[\,\delta^{(\mu\nu}\delta^{\lambda\rho)}-6\,\delta^{(\mu\nu}\hat{e}^{\lambda}\hat{e}^{\rho)}+5\hat{e}^{(\mu}\hat{e}^{\nu}\hat{e}^{\lambda}\hat{e}^{\rho)}],$$

$$\Phi_5^{\mu\nu\lambda\rho\sigma}(\mathbf{e})=\frac{1}{4|\mathbf{e}|^4}\,[3\,\delta^{(\mu\nu}\delta^{\lambda\rho}\hat{e}^{\sigma)}+10\delta^{(\mu\nu}\hat{e}^{\lambda}\hat{e}^{\rho}\hat{e}^{\sigma)} -7\hat{e}^{(\mu}\hat{e}^{\nu}\hat{e}^{\lambda}\hat{e}^{\rho}\hat{e}^{\sigma)}],$$

and

$$\Phi_6^{\mu\nu\lambda\rho\sigma\tau}(\mathbf{e})=\frac{1}{8|\mathbf{e}|^5}\,[-\delta^{(\mu\nu}\delta^{\lambda\rho}\delta^{\sigma\tau)}+15\delta^{(\mu\nu}\delta^{\lambda\rho}\hat{e}^{\sigma}\hat{e}^{\tau)} -35\delta^{(\mu\nu}\hat{e}^{\lambda}\hat{e}^{\rho}\hat{e}^{\sigma}\hat{e}^{\tau)}+21\hat{e}^{(\mu}\hat{e}^{\nu}\hat{e}^{\lambda}\hat{e}^{\rho}\hat{e}^{\sigma}\hat{e}^{\tau)}].$$

Parentheses around superscripts indicates symmetrization (average over permutations) and $\hat{e}$ is the unit vector along e. Only Φ_3 and Φ_4 are needed to compute the free energy itself to two loops. The appearance of Φ_5 and Φ_6 is understood on the basis of the relation

$$\Phi_{n+1}(\mathbf{e})^{\mu_1,\ldots,\mu_{n+1}}=\frac{\partial\Phi_n(\mathbf{e})^{\mu_1,\ldots,\mu_n}}{\partial e^{\mu_{n+1}}}.$$

[1] G. Blatter *et al.*, Rev. Mod. Phys. **66**, 1125 (1994).
[2] G. Grüner, Rev. Mod. Phys. **60**, 1129 (1988).
[3] D. Cule and T. Hwa, Phys. Rev. Lett. **77**, 278 (1996).
[4] C. F. Schmidt, K. Svoboda, N. Lei, I. B. Petsche, L. E. Berman, C. R. Safinya, and G. S. Grest, Science **259**, 952 (1993).
[5] D. H. Boal, Biophys. J. **67**, 521 (1994).
[6] Due to entanglement problems during the process of cytoskeleton extraction and fixing to a substrate, the precise degree of

regularity of the spectrin network is uncertain. From the membrane shear modulus (approximately 10^{-5} N/m) [5], the stress-free filament length (approximately 10^{-7} m), and $k_BT \approx 4 \times 10^{-21}$ N m, the effective dimensionless temperature τ for a Hookean spring model of the network is estimated as $\tau \approx 0.04$. Such a model is therefore in a relatively low-temperature state.

[7] D. Carpentier and P. Le Doussal, cond-mat/9611168; C. Carraro and D. R. Nelson, Phys. Rev. E (to be published).

[8] D. H. Boal, U. Seifert, and J. C. Shillcock, Phys. Rev. E **48**, 4274 (1993).

[9] D. E. Discher, D. H. Boal, and S. K. Boey, Phys. Rev. E **55**, 4762 (1997).

[10] See, for instance, D. R. Nelson and B. I. Halperin, Phys. Rev. B **19**, 2457 (1979).

[11] W. Wintz, R. Everaers, and U. Seifert, J. Phys. I **7**, 1097 (1997). As we have discussed, a critical point seems to be impossible. It should be noted that the simulations in question are done with an ensemble of fixed volume and *fixed shape*. The latter restriction may frustrate collapse of the network so as to force the formation of a superlattice (see Fig. 4 of the present reference). Also, the reported results appear to be restricted to mesh areas above the phase coexistence region, except at very low temperature.

[12] The conventional Lagrangian strain E with respect to the state $\widetilde{M}$ is related by $E=(1/2)[(M\widetilde{M}^{-1})^T(M\widetilde{N}^{-1})-1]$.

[13] A. A. Abrikosov, L. D. Gor'kov, and I. E. Dzyaloshinskii, *Methods of Quantum Field Theory in Statistical Physics* (Dover, New York, 1963).

[14] M. J. Bowick *et al.*, J. Phys. I **6**, 1321 (1996).